



Aligned Magnetohydrodynamics Mixed Convection on Various Base Fluids with Carbon Nanotubes over an Inclined Plate

Nurul Hidayah Ab Raji¹, Nurul Samiha Mohd Shahabudin¹, Noorehan Awang^{2,*}, Mohd Rijal Ilias³, Siti Shuhada Ishak³

¹ Universiti Teknologi MARA (UiTM) Cawangan Perlis, Kampus Arau, 02600 Arau, Perlis, Malaysia

² Universiti Teknologi MARA (UiTM) Cawangan Negeri Sembilan, Kampus Seremban, 70300, Seremban, Negeri Sembilan, Malaysia

³ Universiti Teknologi MARA (UiTM) Shah Alam, 40450 Shah Alam, Selangor, Malaysia

ARTICLE INFO

Article history:

Received 20 November 2022

Received in revised form 19 December 2022

Accepted 1 January 2023

Available online 1 June 2023

Keywords:

Aligned MHD; Carbon Nanotubes; Mixed Convection Flow; Nanofluid; Inclined Plate

ABSTRACT

Analytical and graphical studies are conducted on the impact of carbon nanotubes in aligned magnetohydrodynamics (MHD) mixed convection flow of nanofluid over an inclined plate. Various types of parameters are considered throughout the numerical study with a constant wall temperature. The similarity transformation was implemented to transform the partial differential governing equations into ordinary differential equations. Furthermore, the Fourth-Order Runge Kutta algorithm is built into Maple Software to solve the transformed equations. The analysis shows how various dimensionless parameters; the angle of magnetic field, the interaction of magnetic, the angle of an inclined plate, the volume fraction of nanoparticles, and mixed convection, affect velocity and temperature profiles, as well as how carbon nanotubes with various base fluids affect skin friction and the Nusselt number. As a result, for both types of carbon nanotube nanofluids, SWCNT/kerosene and MWCNT/kerosene, an increase in angle of magnetic field, interaction of magnetic, and mixed convection parameter risen the velocity profile while an increase in angle of inclined plate and volume fraction of nanoparticles enhanced the temperature profile. However, the Nusselt number and skin friction coefficients increase with increasing angle of magnetic field, interaction of magnetic, and mixed convection parameter and decrease with increasing inclined plate angle and volume fraction of nanoparticle. It was found that MWCNT transferred heat more efficiently than SWCNT.

1. Introduction

Nanofluid research has received a lot of interest in recent years. The word “nanofluid” coined by Choi [1] describes a new type of heat transfer fluid based on nanotechnology that exhibits thermal properties superior to that of its base fluids and conventional suspensions of particles. A nanofluid is a diluted suspension of nanoparticles at least one of whose dimensions is smaller than 100 nm. The thermophysical properties of nanofluids are found to be enhanced over those of base fluids like oil or water, including thermal conductivity, thermal diffusivity, viscosity, and convective heat transfer.

* Corresponding author.

E-mail address: noorehan@uitm.edu.my (Noorehan Awang)

<https://doi.org/10.37934/cfdl.15.6.1225>

Thermal conductivity and viscosity are the only two impacts of nanofluids, and they can only be determined by theoretical models or experimental data. Many engineering equipment such as heat exchangers and electronic devices suffer from poor performance and compactness due to the low thermal conductivity of conventional heat transfer fluids, such as water, oil, and ethylene glycol mixtures.

Numerous studies have been conducted using a variety of plates, convection and boundary conditions because of the fascinating nature of nanofluids. In order to investigate how magnetic field, nanolayer conductivity, and nanoparticle diameter affect steady boundary layer nanofluid flow and heat transfer properties, Rana and O. Anwar [2] studied mixed convection flow along an inclined permeable plate. Bhargava and Harish [3] used hybrid approach to explore the behaviour of nanofluid on mixed convective boundary layer flow past an inclined plate embedded in porous medium with predefined surface fluxes. A study on a natural convection of magnetic nanofluid through a fixed vertical plate with convective boundary condition had been conducted by Ilias *et al.*, [4]. In 2022, Rosaidi *et al.*, [5] also looked at the behaviour of aligned magnetohydrodynamics free convection flow of magnetic nanofluid with convective boundary condition by incorporating moving vertical plate.

Over the last 15 years, carbon nanotubes with a nanoscale dimension (1-D) have become well-known. Carbon Nanotube (CNT) was first discovered by Iijima [6] in 1991. Nanotubes are divided into two types by the wall structure of carbon. One is a multi-walled carbon nanotube (MWCNT), and the other is a single-walled carbon nanotube (SWCNT). Furthermore, they determined that CNT deposition might create a thin layer on the surface of the heater, greatly reducing the active nucleation sites on the heater surface. In 2014, Khan *et al.*, [7] proposed a study to analyse the flow and heat transfer of CNT nanofluids through a flat plate. They discovered that the skin friction of single-wall CNTs was higher than that of multi-wall CNTs with all base fluids, while it increased with solid volume fraction due to the higher density of both CNTs. Meanwhile a study by Haq *et al.*, [8] and another by Reddy *et al.*, [9] found that SWCNT produced higher heat transfer rates than MWCNT. Then, Noranuar *et al.*, [10] study the heat transfer of water-based carbon nanotubes in non-coaxial rotation flow affected by MHD and porosity in SWCNTs and MWCNTs solved for the exact solutions by applying the Laplace transform method. They found that both temperature and velocity of the nanofluid as well as enhances the rate of heat transport were increase influence by CNT's volume fraction. Also, SWCNTs provides high values of Nusselt number compared to MWCNTs. Other researcher who studies on CNTs were discuss in [11-13].

Recently, researchers have been attracted to examine fluid flow using mixed convection. Mixed convection is a combination of natural convection and forced convection that occurs when a flow is controlled simultaneously by outer forcing systems and inner volumetric (mass) forces. Wahid *et al.*, [14] discovered that mixed convection parameter improved skin friction and heat transfer rate while so increase the thickness of the thermal boundary layer in their study on hybrid nanofluid passing through a permeable vertical flat plate under the thermal radiation effect. Further, other mixed convection studies [15,16] concurred that the volume fraction of nanoparticles boosts thermal conductivity and improves the thickness of the thermal boundary layer.

MHD is a branch of continuum mechanics that studies how an electrically conducting fluid moves in the presence of a magnetic field. Many industrial uses of MHD include crystal formation, metal casting, and liquid metal cooling blankets for fusion reactors. Ilias *et al.*, [17, 18] investigated the influences of convective boundary condition on the magnetic nanofluids over a flat vertical plate with the presence of a magnetic field and continues the research by considering the inclined plate. They discovered that the value of an aligned magnetic field has a huge impact on velocity, temperature, skin friction coefficient, and Nusselt number. Based on the numerical outcomes from the study

conducted by Syed Ahmad *et al.*, [19] regarding the magnetic field effect, it can be concluded that as the magnetic parameter increases, the velocity, skin friction, and Nusselt number also do so, simultaneously increasing the thickness of the momentum boundary layer. However, as the magnetic parameter increase, it is apparent that the temperature profiles fall, which has an impact on the thickness of the thermal boundary layer as well. In year 2022, Nayan *et al.*, [20] investigates the aligned MHD flow of hybrid nanofluid over a vertical plate through a porous medium followed by Bosli *et al.*, [21] study the aligned MHD natural convection flow and heat transfer of a Casson nanofluid past a vertical plate with convective boundary condition considered by nanoparticles shape. Both studies found that the influence of aligned magnetic field have increase the velocity, skin friction and Nusselt number. In this way, several researchers did the investigation the effect of MHD under different situations [22-30].

To the authors' best knowledge, carbon nanotube was frequently employed in studies that included consideration of the convective boundary condition. Thus, this study is aimed to investigate the effect of carbon nanotube in aligned MHD mixed convection flow of nanofluid through an inclined plate by analysing the velocity and temperature profiles as well as the numerical results on the skin friction and Nusselt number for physical interpretation with constant wall temperature.

2. Mathematical Formulation

This study considers a steady flow of nanofluid over an inclined plate with an aligned and transverse magnetic field in two dimensions, incompressible, laminar, and hydromagnetic mixed convection. The aligned magnetic field, α was introduced to the flow and placed in the free stream temperature T_∞ . Kerosene was used as a base fluid with carbon nanotubes as nanoparticles. The nanoparticle that used in this study were single-wall carbon nanotube (SWCNT) and multi-wall carbon nanotube (MWCNT). The transverse magnetic field considered to be a function of distance from the origin can be defined as $B(x) = B_0 x^{-\frac{1}{2}}$ with $B_0 \neq 0$.

Based on Figure 1 above, B_0 represented the magnetic field strength and the coordinate (x, y) along the plate respectively. It was assumed that there was no slipping occurs between the base fluids and nanoparticles since they were in thermal equilibrium. The effects of dissipation and radiation due to viscous dissipation were being ignored.

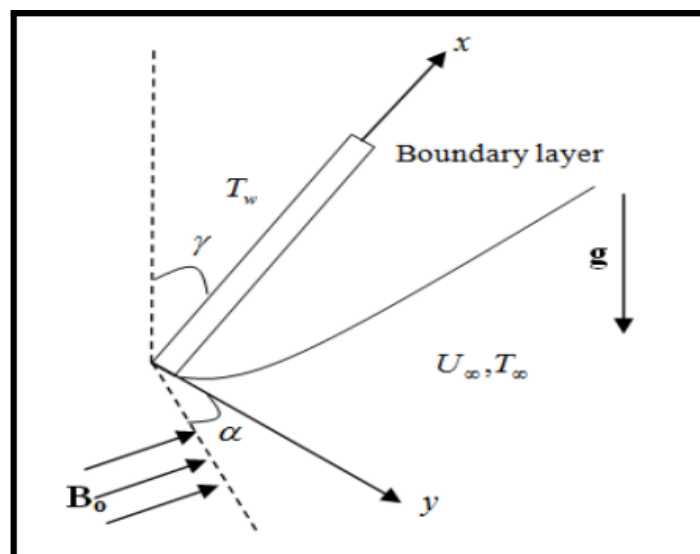


Fig. 1. Geometry of the problem [13]

Together with the assumptions of Boussinesq and boundary layer approximation, the equation of MHD boundary layer flow can be expressed as [17]:

$$\frac{\partial u}{\partial x} + \frac{\partial v}{\partial y} = 0 \tag{1}$$

$$u \frac{\partial u}{\partial x} + v \frac{\partial u}{\partial y} = \frac{\mu_{nf}}{\rho_{nf}} \frac{\partial^2 u}{\partial y^2} + \frac{(\rho\beta)_{nf}}{\rho_{nf}} g \cos \gamma (T - T_\infty) - \frac{\alpha\beta^2(x)}{\rho_{nf}} \sin^2 \alpha (U - U_\infty) \tag{2}$$

$$u \frac{\partial T}{\partial x} + v \frac{\partial T}{\partial y} = \alpha_{nf} \frac{\partial^2 T}{\partial y^2} \tag{3}$$

While the boundary conditions for this study are as follows [17]:

$$\begin{aligned} u(x, 0) = 0, \quad v(x, 0) = 0, \quad T(x, 0) = T_w \\ U(x, \infty) = U_\infty, \quad T(x, \infty) = T_\infty \end{aligned} \tag{4}$$

where u and v are refers to x (along the plate) and y (normal to the plate) components of velocity respectively. T is the temperature of magnetic nanofluid, T_w is the ambient temperature of the nanofluid, U_∞ is the constant free stream velocity and σ is the electrical conductivity. The effective properties of nanofluids may be expressed in term of the properties of base fluids, nanofluid, and the volume fraction of solid nanofluid as follows:

$$\begin{aligned} \rho_{nf} &= (1 - \phi)\rho_f - \phi\rho_s, \\ \mu_{nf} &= \frac{\mu_f}{(1 - \phi)^{2.5}}, \quad (\rho C_p)_{nf} = (1 - \phi)(\rho C_p)_f + \phi(\rho C_p)_s, \\ (\rho\beta)_{nf} &= (1 - \phi)(\rho\beta)_f + \phi(\rho\beta)_s, \quad \alpha_{nf} = \frac{k_{nf}}{(\rho C_p)_{nf}}, \\ \frac{k_{nf}}{k_f} &= \frac{1 - \phi + 2\phi \left(\frac{k_{CNT}}{k_{CNT} - k_f} \right) \ln \left(\frac{k_{CNT} + k_f}{2k_f} \right)}{1 - \phi + 2\phi \left(\frac{k_f}{k_{CNT} - k_f} \right) \ln \left(\frac{k_{CNT} + k_f}{2k_f} \right)}, \end{aligned} \tag{5}$$

where ρ_{nf} is the effective density, ϕ is the solid volume fraction, ρ_f and ρ_s are the densities of pure fluid and nanoparticles, respectively, μ_f is the dynamic viscosity of the base fluid, μ_{nf} is the effective dynamic viscosity, $(\rho C_p)_{nf}$ is the heat capacity of nanofluids, $(\rho C_p)_f$ is specific heat parameters of the base fluid, $(\rho C_p)_s$ is specific heat parameter of nanoparticles, $(\rho\beta)_{nf}$ is the thermal expansion coefficient, α_{nf} is the thermal diffusivity of the nanofluids, k_{nf} is the thermal conductivity of nanofluids, k_f is the thermal conductivity of the fluids.

By introducing a stream function $\psi(x, y)$, the continuity equation in Eq. (1) is satisfied. So, we can write u and v as:

$$u = \frac{\partial \psi}{\partial y} \text{ and } v = \frac{\partial \psi}{\partial x} \tag{6}$$

The following similarity variables are introduced to solve the governing equation in Eq. (1) to Eq. (3), as in the study by Illias *et al.*, [13]

$$\eta = y \left(\frac{U_\infty}{\nu_f x} \right)^{\frac{1}{2}} = \frac{y}{x} \sqrt{\text{Re}_x} = \frac{y}{x} \left(\frac{U_\infty x}{\nu_f} \right)^{\frac{1}{2}}, \quad \psi = \nu_f \sqrt{\text{Re}_x} f(\eta), \quad \theta(\eta) = \frac{T - T_\infty}{T_w - T_\infty} \tag{7}$$

where η is the similarity variable, $\text{Re}_x = \frac{U_\infty x}{\nu_f}$ represented as Local Reynolds number, $f(\eta)$ and $\theta(\eta)$ were indicates the non-dimensional stream function and temperature respectively.

By substitute Eq. (5), Eq. (6) and Eq. (7) into Eq. (2) and Eq. (3), the following non-linear system of ordinary differential equations were obtained:

$$f'''(\eta) + (1-\phi)^{2.5} \left[(1-\phi) + \phi \frac{(\rho\beta)_s}{(\rho\beta)_f} \right] \theta(\eta) \lambda \cos \gamma - (1-\phi)^{2.5} M \sin^2 \alpha (f'(\eta) - 1) + \frac{(1-\phi)^{2.5}}{2} \left[(1-\phi) + \phi \frac{\rho_s}{\rho_f} \right] (f(\eta) f''(\eta)) = 0 \tag{8}$$

$$\frac{k_{nf}}{k_f} \theta''(\eta) + \frac{\text{Pr}}{2} \left[(1-\phi) + \phi \frac{(\rho C \rho)_s}{(\rho C \rho)_f} \right] f(\eta) \theta'(\eta) = 0 \tag{9}$$

The boundary conditions derived by using Eq. (4) were as follows:

$$\begin{aligned} f'(0) = 0, \quad f(0) = 0, \quad \theta(0) = 0 \\ f'(\infty) = 1, \quad \theta(\infty) = 0 \quad \text{as } \eta \rightarrow \infty \end{aligned} \tag{10}$$

where primes are denoted differentiations with respect to η , α is inclination angle of magnetic field, $\lambda = \frac{g\beta_f(T_w - T_\infty)x}{U_\infty^2}$ is mixed convection parameter, $M = \frac{\sigma B_0^2}{\rho_f(U_\infty)}$ is magnetic interaction parameter, γ is angle of inclined plate, and $\text{Pr} = \frac{(\mu C_p)}{k_f}$ is the Prandtl number.

The numerical results are discussed based on the skin friction coefficient, C_f at the surface of the plate and Nusselt number, Nu_x which are defined as:

$$C_f = \frac{\tau_w}{\rho_f U_\infty^2}, \quad Nu_x = \frac{xq_w}{k_f(T_w - T_\infty)} \quad (11)$$

where τ_w refer to the wall skin friction and q_w defined as the prescribe heat flux which given by:

$$\tau_w = \mu_{nf} \left(\frac{\partial u}{\partial y} \right)_{y=0}, \quad q_w = -k_{nf} \left(\frac{\partial T}{\partial y} \right)_{y=0} \quad (12)$$

By substitute Eq. (7) and Eq. (12) into Eq. (11), the solutions obtained were as follows:

$$\frac{C_f}{(\text{Re}_x)^{\frac{1}{2}}} = \frac{f''(0)}{(1-\phi)^{2.5}}, \quad \frac{Nu_x}{(\text{Re}_x)^{\frac{1}{2}}} = -\frac{k_{nf}}{k_f} \theta'(\eta) \quad (13)$$

The thermophysical properties of the base fluid and the solid nanoparticles are given in Table 1.

Table 1
 Thermophysical properties of base fluids and nanoparticle [31, 32]

| | | Thermophysical Properties | | | |
|--------------|-----------------|-----------------------------|--|---|--|
| | | ρ (kg/m ³) | c_p (kg ⁻¹ /k ⁻¹) | k (Wm ⁻¹ k ⁻¹) | $(\beta \times 10^{-5} \text{k}^{-1})$ |
| Base Fluid | Water | 997 | 4179 | 0.613 | 21 |
| | Kerosene Oil | 783 | 2090 | 0.145 | 99 |
| | Engine Oil | 884 | 1910 | 0.114 | 70 |
| | Ethylene Glycol | 1132 | 2349 | 0.258 | 57 |
| Nanoparticle | SWCNT | 2600 | 425 | 6600 | 27 |
| | MWCNT | 1600 | 796 | 3000 | 44 |

3. Method of Solution

The nonlinear equations Eq. (8) and Eq. (9) cannot be solved analytically. The relative robust computer algebra software Maple 20 is used to derive numerical solutions subject to the boundary condition (10). The dsolve command in this software solves boundary value problems numerically using a fourth-order Runge Kutta Method as the default.

The current research's results were compared to the results of a prior study that to illustrate the dependability of the numerical results and the consistency of the inquiry. From Table 2, we can see that the data produced has a good agreement with the previous researchers.

Table 2
 Comparison results of static vertical plate, ($\gamma = 0^\circ$) on skin friction and Nusselt number for α in Fe_3O_4 -kerosene ferrofluids

| α | M | ϕ | Gr_x | Bi_x | Skin Friction Coefficient | | Nusselt Number | |
|----------|-----|--------|--------|--------|---------------------------|---------------|---------------------------|---------------|
| | | | | | Ilias <i>et al.</i> , [4] | Present Study | Ilias <i>et al.</i> , [4] | Present Study |
| 0° | 1 | 0.1 | 0.1 | 0.1 | 0.4794 | 0.4794 | 0.1178 | 0.1178 |
| 45° | | | | | 0.9245 | 0.9245 | 0.1198 | 0.1198 |
| 70° | | | | | 1.1601 | 1.1600 | 0.1204 | 0.1207 |
| 90° | | | | | 1.2233 | 1.2233 | 0.1205 | 0.1205 |

4. Result and Discussion

The effects of carbon nanotubes and dimensionless parameters on velocity and temperature profiles were graphically illustrated, and the effects on skin friction and Nusselt number were tabulated. The Prandtl numbers are assumed to be 21, 6.2, 100, and 137.48 for the base fluids, which are kerosene, water, engine oil, and ethylene glycol, respectively. We fit the nondimensional values as follows for numerical computation, $\alpha = 90^\circ$, $M = 1$, $\gamma = 45^\circ$, $\phi = 0.1$, and $\lambda = 1$ unless otherwise mentioned. In this study, $\gamma = 0^\circ$ denotes the static vertical plate while $\gamma = 90^\circ$ denotes static horizontal plate.

Figure 2 displays the effect of carbon nanotubes with different base fluids (kerosene, water, engine oil, and ethylene glycol) on velocity and temperature profiles, while Table 3 displays the effect's numerical value on skin friction and Nusselt number. Furthermore, Figures 3 to 7 shows how the velocity and temperature profiles change as the value of dimensionless parameters, α , M , γ , ϕ , and λ varies. The effect of dimensionless parameters on skin friction and Nusselt number are discussed further in Table 4.

4.1 Effect of Carbon Nanotubes on Various Base Fluids

Figure 2(a) and Figure 2(b) illustrate the effect of carbon nanotubes on the velocity and temperature profiles for both SWCNT and MWCNT. All these results are analysed for kerosene, water, engine oil, and ethylene glycol. It shows that carbon nanotubes have different influences on velocity and temperature profiles. Figure 2(a) shows that velocity reached the highest level when it became to SWCNT/water and MWCNT/water. The velocity bottomed out when it became to SWCNT/ethylene glycol and MWCNT/ethylene glycol. The same goes for the temperature profile that SWCNT/water and MWCNT/water reached a peak while SWCNT/ethylene glycol and MWCNT/ethylene glycol were at the lowest level on the temperature profile. For each type of base fluids, fluids that contained SWCNT had the highest velocity and temperature compared to fluids that contained MWCNT.

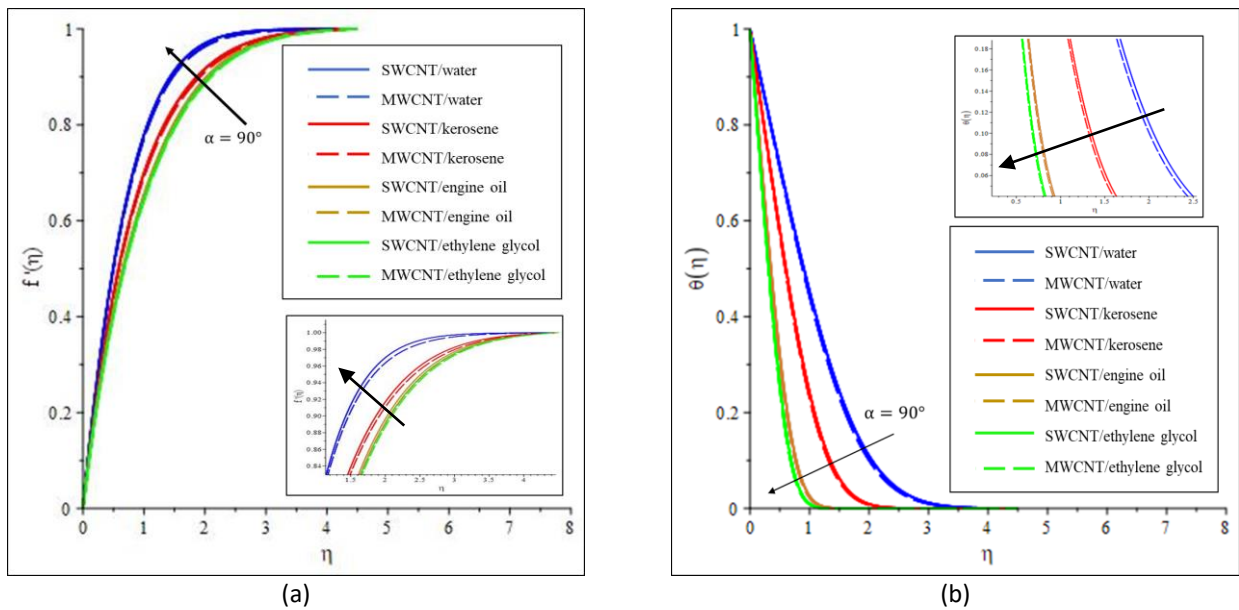


Fig. 2. Effect of carbon nanotubes on (a) velocity and (b) temperature profiles

The numerical results of the effect of carbon nanotubes on skin friction coefficient and Nusselt number are shown in Table 3. Here we can see that the highest wall shear stress occurred for SWCNT/water followed by MWCNT/water because both of these nanofluids have highest value of skin friction. While SWCNT/ethylene glycol and MWCNT/ethylene glycol had the lowest impact on skin friction. As for the Nusselt number, MWCNT/ethylene glycol has the highest value followed by SWCNT/ethylene glycol. Carbon nanotubes-based water have the lowest value of Nusselt number. For each type of base fluids, fluids that contained SWCNT had the highest value of skin friction coefficient and the lowest value of Nusselt number. In comparison of carbon nanotubes, MWCNT has greater impact on heat transfer compared to SWCNT while SWCNT has greatest value of skin friction.

Table 3
 Effects of carbon nanotubes on skin friction and Nusselt number with various base fluids

| Base Fluid | Skin Friction | | Nusselt Number | |
|-----------------|---------------|---------|----------------|---------|
| | SWCNT | MWCNT | SWCNT | MWCNT |
| Water | 1.71666 | 1.70533 | 0.76026 | 0.77765 |
| Kerosene | 1.52679 | 1.51649 | 1.13414 | 1.15839 |
| Engine Oil | 1.42520 | 1.41569 | 1.94163 | 1.98211 |
| Ethylene Glycol | 1.40161 | 1.39365 | 2.17292 | 2.21804 |

4.2 Effect of Dimensionless Parameters

Figure 3(a) and Figure 3(b) depict the effect of α in velocity and temperature profiles with a constant value of M , γ , ϕ , and λ . These two figures show that α has different influences on velocity and temperature profiles. As observed, the SWCNT/kerosene has the highest effect on velocity and temperature compared to MWCNT/kerosene. As α increases the velocity profile increases while the temperature profile decreases. An increasing in α reduces both of the momentum boundary layer and the thermal boundary layer thicknesses.

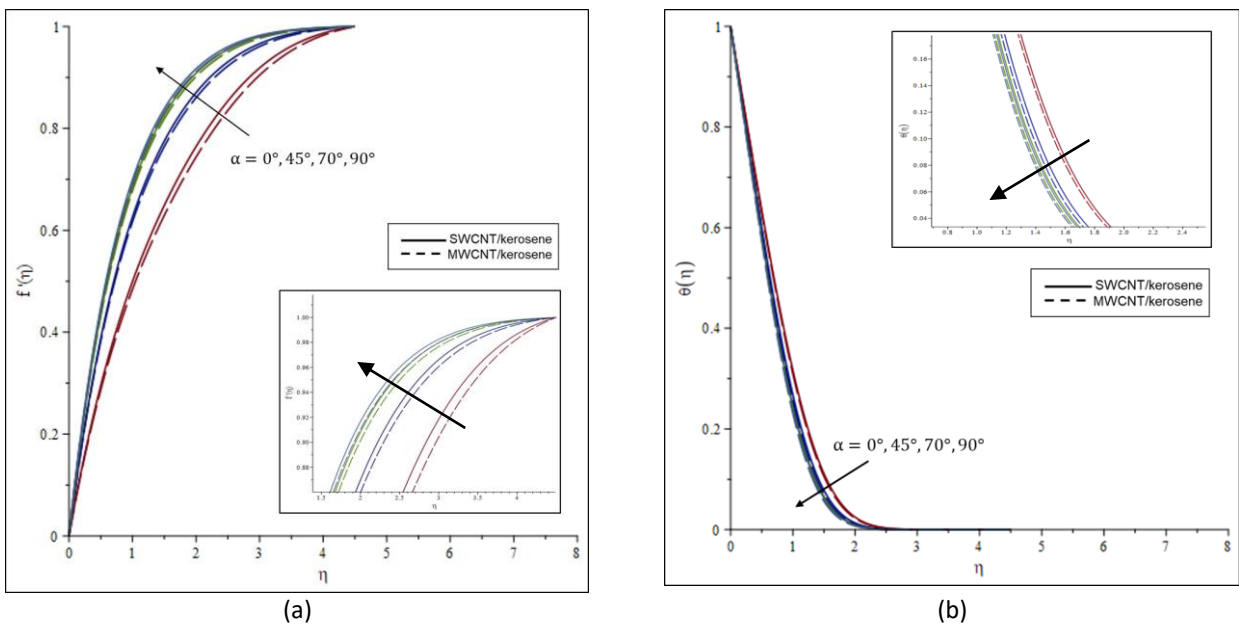


Fig. 3. Effect of α on (a) velocity and (b) temperature profiles

Figure 4(a) and Figure 4(b) illustrate the impact of M on velocity profiles and temperature profiles with different values of α , γ , ϕ , and λ . In figure 4(a) the curves that represented $M = 1, 2, 3$, for both types of fluids, the curves were slightly the same compared to when $M = 0$. The velocity profiles increase as a result of the strengthening in M while the temperature profiles fall. The magnetic field accelerates the nanofluid, which is slowed down by viscous force. As a result, as the value of M increases, the velocity profiles of the nanofluid increase and the thickness of the momentum boundary layer reduces, while the temperature profiles of the nanofluid increase and the thickness of the thermal boundary layer decreases.

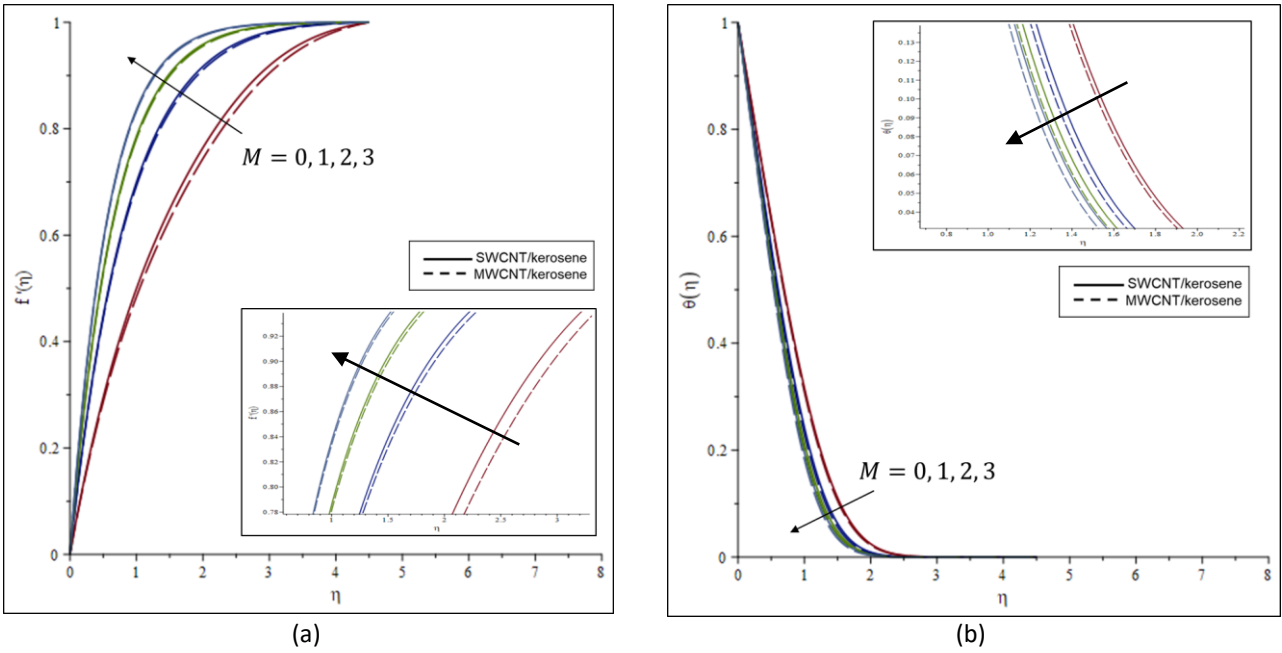


Fig. 4. Effect of M on (a) velocity profiles and (b) temperature profiles

Effect of γ on velocity profiles and temperature profiles represented in Figure 5(a) and Figure 5(b). As seen in Figure 5(a) and Figure 5(b), γ has no substantial impact on velocity and temperature profiles. In Figure 5(a) gravitational effects were minimum at $\gamma = 90^\circ$, and maximum at $\gamma = 0^\circ$. In the case of $\gamma = 90^\circ$ where $\cos(90^\circ) = 0$, buoyancy effects are eliminated because the gravity field is normal to the plate surface and has no effect on the flow. As γ increases, $\cos(\gamma)$ decreases. Consequently, when the value of γ increases, the buoyancy effect is diminished. Observed that SWCNT had greater influence on velocity profiles than MWCNT. With an increase in γ , the velocity profiles decrease and temperature profiles increase. As a result, the momentum boundary layer and the thermal boundary layer thickness increases respectively.

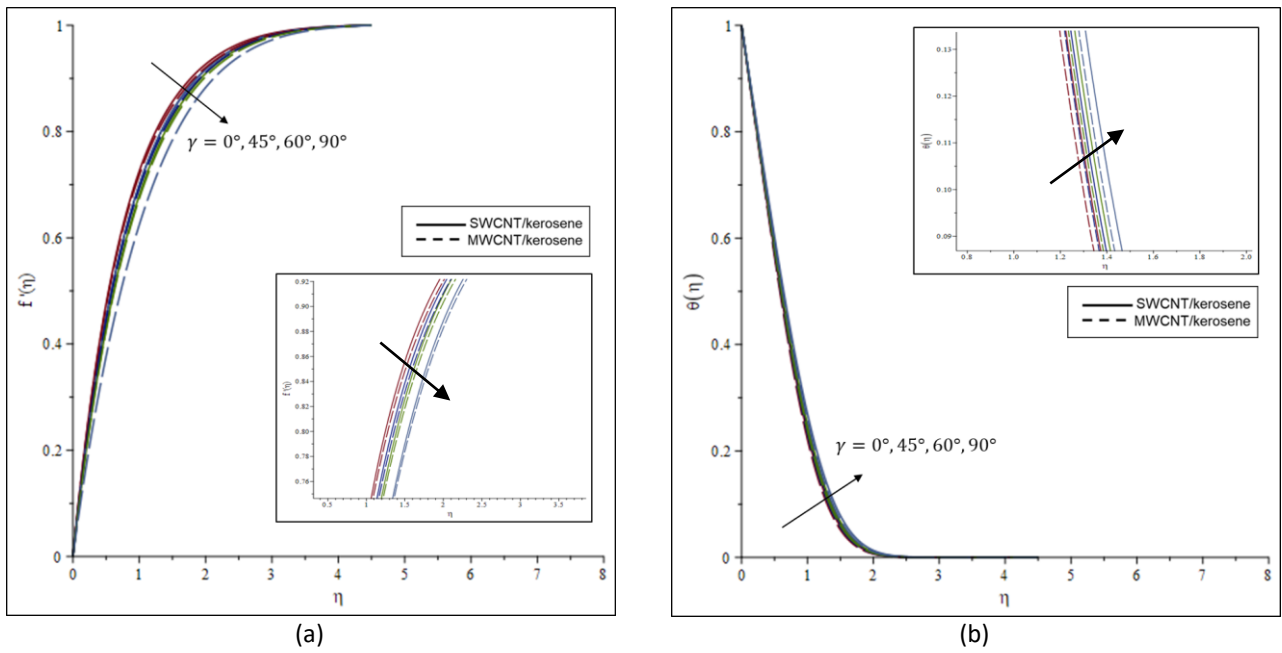


Fig. 5. Effect of γ on (a) velocity profiles and (b) temperature profiles

Effect of ϕ on velocity profiles and temperature profiles was illustrated in Figure 6(a) and Figure 6(b). The ϕ had significantly impacted the velocity profile when $\phi = 0.2$ because this value gives the lowest velocity. The velocity profile reduces as ϕ increases because the nanofluids become viscous as the number of nanoparticles increases. Therefore, momentum boundary layer increases. As shown in Figure 6(b), increasing in ϕ improves the temperature profile by increasing the temperature as nanoparticles collide with the plate's surface and it also increases the thermal boundary layer thickness. According to logic, the thermal conductivity of the nanofluids will increase as ϕ increases, raising the fluids' temperature.

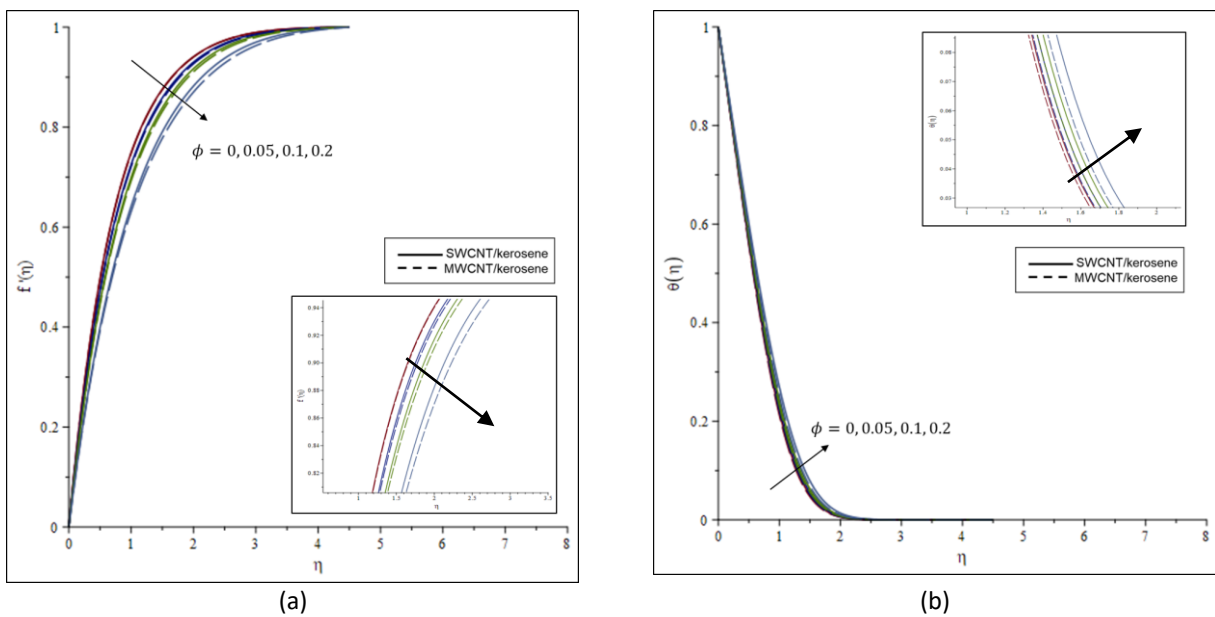


Fig. 6. Effect of ϕ on (a) velocity and (b) temperature profiles

Figure 7(a) and Figure 7(b) illustrated the impact of λ on velocity and temperature profiles with constant value of α , M , γ , and ϕ . The velocity profile increased as increased in λ while the temperature profile decreased as λ increased. However, SWCNT/kerosene had more effects compared to MWCNT/kerosene on velocity profile whereas SWCNT/kerosene more effects than MWCNT/kerosene on temperature profile. As a result, the momentum boundary layer and thermal boundary layer thickness decreased as increased in λ .

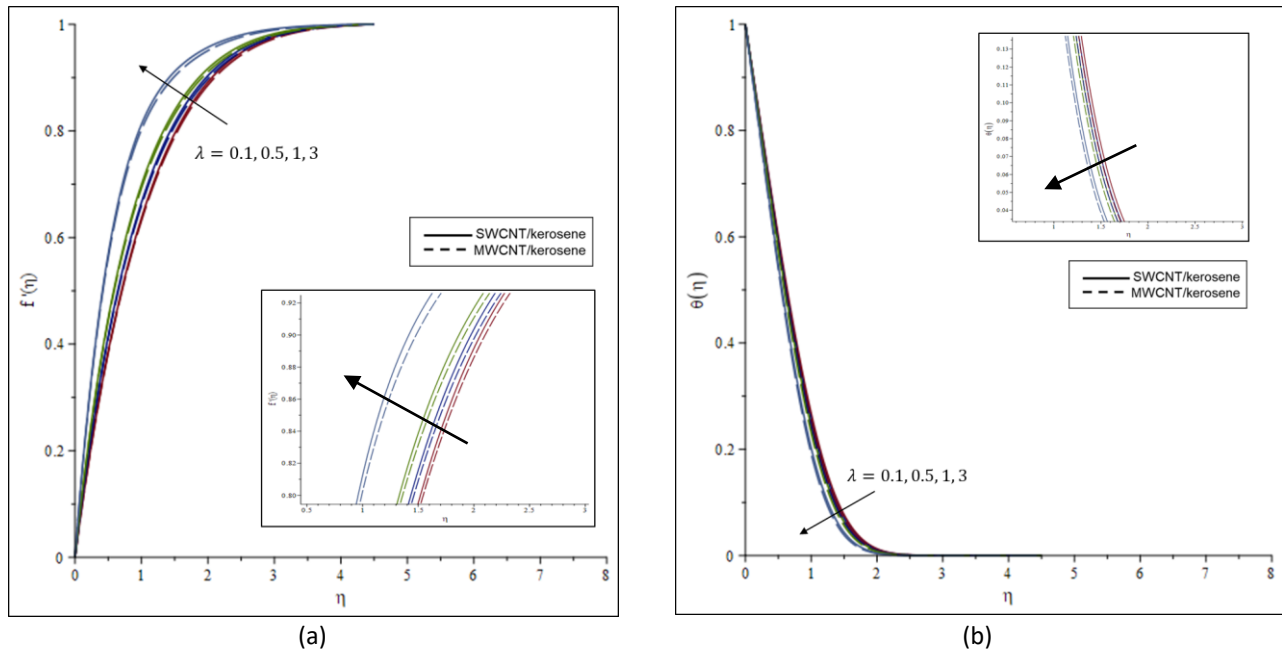


Fig. 7. Effect of λ on (a) velocity and (b) temperature profile

As depicts in Table 4, the skin friction coefficient and Nusselt number rise as α , M , and λ increases. Meanwhile as the value of γ and ϕ increase, the value of skin friction coefficient and Nusselt number falls. In comparison to all dimensionless parameters, highest wall shear stress occurred when M was increased for both SWCNT and MWCNT on skin friction coefficient. It is observed that α and M gave significant impact to skin friction. For all values of dimensionless parameter, SWCNT/kerosene had the highest value of skin friction coefficient compared to MWCNT/kerosene. It also noticed that the MWCNT/kerosene had the highest value of Nusselt number compared to SWCNT/kerosene.

Table 4
 Effects of dimensionless parameters on skin friction and Nusselt number

| α | M | γ | ϕ | λ | Skin Friction | | Nusselt Number | |
|----------|-----|----------|--------|-----------|---------------|----------|----------------|----------|
| | | | | | SWCNT | MWCNT | SWCNT | MWCNT |
| | | | | | Kerosene | Kerosene | Kerosene | Kerosene |
| 0° | 1 | 45° | 0.1 | 1 | 0.92297 | 0.90094 | 0.98337 | 0.99659 |
| | | | | | 1.2697 | 1.25542 | 1.07844 | 1.09931 |
| | | | | | 1.47217 | 1.46042 | 1.12269 | 1.14629 |
| | | | | | 1.52776 | 1.51656 | 1.13377 | 1.15799 |
| 90° | 1 | 45° | 0.1 | 1 | 0.92297 | 0.90094 | 0.98337 | 0.99659 |
| | | | | | 1.52776 | 1.51656 | 1.13377 | 1.15799 |
| | | | | | 1.93103 | 1.92271 | 1.20347 | 1.23131 |
| | | | | | 2.25673 | 2.24985 | 1.24940 | 1.27940 |
| 90° | 1 | 0° | 0.1 | 1 | 1.65619 | 1.64322 | 1.15638 | 1.18096 |
| | | | | | 1.52776 | 1.51656 | 1.13377 | 1.15799 |
| | | | | | 1.43499 | 1.42508 | 1.11688 | 1.14085 |
| | | | | | 1.20325 | 1.19662 | 1.07241 | 1.09572 |
| 90° | 1 | 45° | 0 | 1 | 1.75364 | 1.75064 | 1.18892 | 1.20283 |
| | | | | | 1.63970 | 1.63239 | 1.16173 | 1.18088 |
| | | | | | 1.52776 | 1.51656 | 1.13377 | 1.15799 |
| | | | | | 1.30954 | 1.29265 | 1.07530 | 1.10911 |
| 90° | 1 | 45° | 0.1 | 0.1 | 1.23677 | 1.22966 | 1.07906 | 1.10246 |
| | | | | | 1.36833 | 1.35935 | 1.10444 | 1.12821 |
| | | | | | 1.52776 | 1.51656 | 1.13377 | 1.15799 |
| | | | | | 2.12354 | 2.10422 | 1.23226 | 1.25810 |

5. Conclusions

The study is carried out to investigate the effect of carbon nanotubes with various base fluids and impact of dimensionless parameters in aligned magnetohydrodynamics mixed convection flow of nanofluid through an inclined plate with constant wall temperature as the boundary condition. The analysis on the impact of dimensionless parameters had been made to SWCNT/kerosene and MWCNT/kerosene nanofluids. The solution of the problems was numerically solved with the help of Fourth-Order Runge Kutta Method and the results are presented graphically and tabulated.

The following conclusion can be drawn from the results obtained:

- i. The velocity profile increases with an increase in α , M , and λ whereas it decreases with an increase in γ and ϕ .
- ii. The temperature profile decreases with an increase in α , M , and λ whereas it increases with an increase in γ and ϕ .
- iii. An increase in α , M , and λ decrease the momentum boundary layer thickness while an increase in γ and ϕ rise the momentum boundary layer thickness.
- iv. An increase in α , M , and λ reduces the thickness of the thermal boundary layer, while an increase in γ and ϕ increases the thickness of the thermal boundary layer.
- v. The Nusselt and local skin friction coefficients rise as α , M , and λ increase and decrease as an increase in γ and ϕ .

- vi. The skin friction coefficients have the highest value when it comes to SWCNT with various base fluids while the Nusselt number has the highest value for MWCNT with various base fluids.
- vii. In general, MWCNT improve heat transfer rate compared to SWCNT.

Acknowledgement

The authors extend their appreciation to Universiti Teknologi MARA for funding this work through Geran Penyelidikan MyRA (GPM) under grant number 600-RMC 5/3/GPM (041/2022).

References

- [1] Choi, S. US, and Jeffrey A. Eastman. *Enhancing thermal conductivity of fluids with nanoparticles*. No. ANL/MSD/CP-84938; CONF-951135-29. Argonne National Lab.(ANL), Argonne, IL (United States), 1995.
- [2] Rana, Puneet, and O. Anwar Bég. "Mixed convection flow along an inclined permeable plate: effect of magnetic field, nanolayer conductivity and nanoparticle diameter." *Applied Nanoscience* 5 (2015): 569-581. <https://doi.org/10.1007/s13204-014-0352-z>
- [3] Bhargava, Rama, and Harish Chandra. "Hybrid numerical solution of mixed convection boundary layer flow of nanofluid along an inclined plate with prescribed surface fluxes." *International Journal of Applied and Computational Mathematics* 3 (2017): 2909-2928. <https://doi.org/10.1007/s40819-016-0278-0>
- [4] Ilias, Mohd Rijal, Noraihan Afiqah Rawi, and Sharidan Shafie. "Natural convection of ferrofluid from a fixed vertical plate with aligned magnetic field and convective boundary condition." *Malaysian Journal of Fundamental and Applied Sciences* 13, no. 3 (2017). <https://doi.org/10.11113/mjfas.v13n3.651>
- [5] Rosaidi, Nor Alifah, Nurul Hidayah Ab Raji, Siti Nur Hidayatul Ashikin Ibrahim, and Mohd Rijal Ilias. "Aligned magnetohydrodynamics free convection flow of magnetic nanofluid over a moving vertical plate with convective boundary condition." *Journal of Advanced Research in Fluid Mechanics and Thermal Sciences* 93, no. 2 (2022): 37-49. <https://doi.org/10.37934/arfmts.93.2.3749>
- [6] Iijima, Sumio. "Helical microtubules of graphitic carbon." *nature* 354, no. 6348 (1991): 56-58. <https://doi.org/10.1038/354056a0>
- [7] Khan, W. A., Z. H. Khan, and M. Rahi. "Fluid flow and heat transfer of carbon nanotubes along a flat plate with Navier slip boundary." *Applied Nanoscience* 4 (2014): 633-641. <https://doi.org/10.1007/s13204-013-0242-9>
- [8] Haq, Rizwan Ul, Irfan Rashid, and Z. H. Khan. "Effects of aligned magnetic field and CNTs in two different base fluids over a moving slip surface." *Journal of Molecular Liquids* 243 (2017): 682-688. <https://doi.org/10.1016/j.molliq.2017.08.084>
- [9] Reddy, S. R. R., P. Bala Anki Reddy, and Ali J. Chamkhab. "MHD flow analysis with water-based CNT nanofluid over a non-linear inclined stretching/shrinking sheet considering heat generation." *CHEMICAL ENGINEERING* 71 (2018).
- [10] Noranuar, Wan Nura'in Nabilah, Ahmad Qushairi Mohamad, Sharidan Shafie, Ilyas Khan, Mohd Rijal Ilias, and Lim Yeou Jiann. "Analysis of Heat Transfer in Non-Coaxial Rotation of Newtonian Carbon Nanofluid Flow with Magnetohydrodynamics and Porosity Effects." *21st Century Nanostructured Materials* (2021): 93. <https://doi.org/10.5772/intechopen.100623>
- [11] Noranuar, Wan Nura'in Nabilah, Ahmad Qushairi Mohamad, Sharidan Shafie, Ilyas Khan, Mohd Rijal Ilias, and Lim Yeou Jiann. "Analysis of Heat Transfer in Non-Coaxial Rotation of Newtonian Carbon Nanofluid Flow with Magnetohydrodynamics and Porosity Effects." *21st Century Nanostructured Materials* (2021): 93.
- [12] Alsagri, Ali Sulaiman, Saleem Nasir, Taza Gul, Saeed Islam, K. S. Nisar, Zahir Shah, and Ilyas Khan. "MHD thin film flow and thermal analysis of blood with CNTs nanofluid." *Coatings* 9, no. 3 (2019): 175. <https://doi.org/10.3390/coatings9030175>
- [13] Hossain, Rumman, A. K. Azad, Md Jahid Hasan, and M. M. Rahman. "Radiation effect on unsteady MHD mixed convection of kerosene oil-based CNT nanofluid using finite element analysis." *Alexandria Engineering Journal* 61, no. 11 (2022): 8525-8543. <https://doi.org/10.1016/j.aej.2022.02.005>
- [14] Wahid, Nur Syahirah, Norihan Md Arifin, Najiyah Safwa Khashi'ie, Ioan Pop, Norfifah Bachok, and Mohd Ezad Hafidz Hafidzuddin. "MHD mixed convection flow of a hybrid nanofluid past a permeable vertical flat plate with thermal radiation effect." *Alexandria Engineering Journal* 61, no. 4 (2022): 3323-3333. <https://doi.org/10.1016/j.aej.2021.08.059>
- [15] P. Suriyakumar "Mixed Convective Hydromagnetic Stagnation Point Flow of Nanofluid over an Inclined Stretching Plate with Prescribed Surface Heat Flux." *International Journal of Trend in Scientific Research and Development (ijtsrd)* 4 | no. 3 (2020): 905-914.

- [16] Anjali Devi, S. P., and P. Suriyakumar. "Hydromagnetic mixed convective nanofluid slip flow past an inclined stretching plate in the presence of internal heat absorption and suction." *Journal of Applied Fluid Mechanics* 9, no. 3 (2016): 1409-1419. <https://doi.org/10.18869/acadpub.jafm.68.228.24194>
- [17] Ilias, Mohd Rijal, Noraihan Afiqah Rawi, and Sharidan Shafie. "Steady aligned MHD free convection of Ferrofluids flow over an inclined plate." *Journal of Mechanical Engineering (JMEchE)* 14, no. 2 (2017): 1-15.
- [18] Ilias, Mohd Rijal, Noraihan Afiqah Rawi, Noor Hidayah Mohd Zaki, and Sharidan Shafie. "Aligned mhd magnetic nanofluid flow past a static wedge." *Int. J. Eng. Technol* 7, no. 3.28 (2018): 28-31. <https://doi.org/10.14419/ijet.v7i3.28.20960>
- [19] Ahmad, Sayyid Zainal Abidin Syed, Wan Azmi Wan Hamzah, Mohd Rijal Ilias, Sharidan Shafie, and Gholamhassan Najafi. "Unsteady MHD Boundary Layer Flow and Heat Transfer of Ferrofluids Over A Horizontal Flat Plate with Leading Edge Accretion." *Journal of Advanced Research in Fluid Mechanics and Thermal Sciences* 59, no. 2 (2019): 163-181.
- [20] Nayan, Asmahani, Nur Izzatie Farhana Ahmad Fauzan, Mohd Rijal Ilias, Shahida Farhan Zakaria, and Noor Hafizah Zainal Aznam. "Aligned Magnetohydrodynamics (MHD) Flow of Hybrid Nanofluid Over a Vertical Plate Through Porous Medium." *Journal of Advanced Research in Fluid Mechanics and Thermal Sciences* 92, no. 1 (2022): 51-64. <https://doi.org/10.37934/arfmts.92.1.5164>
- [21] Bosli, Fazillah, Alia Syafiqah Suhaimi, Siti Shuhada Ishak, Mohd Rijal Ilias, Amirah Hazwani Abdul Rahim, and Anis Mardiana Ahmad. "Investigation of Nanoparticles Shape Effects on Aligned MHD Casson Nanofluid Flow and Heat Transfer with Convective Boundary Condition." *Journal of Advanced Research in Fluid Mechanics and Thermal Sciences* 91, no. 1 (2022): 155-171. <https://doi.org/10.37934/arfmts.91.1.155171>
- [22] Makinde, O. D., W. A. Khan, and Z. H. Khan. "Buoyancy effects on MHD stagnation point flow and heat transfer of a nanofluid past a convectively heated stretching/shrinking sheet." *International Journal of Heat and Mass Transfer* 62 (2013): 526-533. <https://doi.org/10.1016/j.ijheatmasstransfer.2013.03.049>
- [23] Reddy, P. Sudarsana, and P. Sreedevi. "MHD boundary layer heat and mass transfer flow of nanofluid through porous media over inclined plate with chemical reaction." *Multidiscipline Modeling in Materials and Structures* 17, no. 2 (2021): 317-336. <https://doi.org/10.1108/MMMS-03-2020-0044>
- [24] Ramli, N., S. Ahmad, and I. Pop. "MHD forced convection ow and heat transfer of ferro fluids over a moving at plate with uniform heat flux and second-order slip effects." *Scientia Iranica* 25, no. 4 (2018): 2186-2197. <https://doi.org/10.1063/1.4995847>
- [25] Zafar, Azhar Ali, Jan Awrejcewicz, Grzegorz Kudra, Nehad Ali Shah, and Se-Jin Yook. "Magneto-free-convection flow of a rate type fluid over an inclined plate with heat and mass flux." *Case Studies in Thermal Engineering* 27 (2021): 101249. <https://doi.org/10.1016/j.csite.2021.101249>
- [26] Muzakkar, M. Z., A. A. Umar, I. Ilham, Z. Saputra, L. Zulfikar, M. Maulidiyah, D. Wibowo, R. Ruslan, and M. Nurdin. "Chalcogenide material as high photoelectrochemical performance Se doped TiO₂/Ti electrode: Its application for Rhodamine B degradation." In *Journal of Physics: Conference Series*, vol. 1242, no. 1, p. 012016. IOP Publishing, 2019. <https://doi.org/10.1088/1742-6596/890/1/012054>
- [27] Ismail, Nur Suhaida Aznidar, Ahmad Sukri Abd Aziz, Mohd Rijal Ilias, and Siti Khuzaimah Soid. "Mhd boundary layer flow in double stratification medium." In *Journal of Physics: Conference Series*, vol. 1770, no. 1, p. 012045. IOP Publishing, 2021. <https://doi.org/10.1088/1742-6596/1770/1/012045>
- [28] Khashi'ie, Najiyah Safwa, Norihan Md Arifin, Ezad Hafidz Hafidzuddin, Nadiyah Wah, and Mohd Rijal Ilias. "Magneto-hydrodynamics (MHD) flow and heat transfer of a doubly stratified nanofluid using Cattaneo-Christov model." *Universal Journal of Mechanical Engineering* 7, no. 4 (2019): 206-214. <https://doi.org/10.13189/ujme.2019.070410>
- [29] Ismail, M. A., N. F. Mohamad, M. R. Ilias, and S. Shafie. "MHD Effect on Unsteady Mixed Convection Boundary Layer Flow past a Circular Cylinder with Constant Wall Temperature." In *Journal of Physics: Conference Series*, vol. 890, no. 1, p. 012054. IOP Publishing, 2017. <https://doi.org/10.1088/1742-6596/890/1/012054>
- [30] Ahmad, Sayyid Zainal Abidin Syed, Wan Azmi Wan Hamzah, Mohd Rijal Ilias, Sharidan Shafie, and Gholamhassan Najafi. "Unsteady MHD Boundary Layer Flow and Heat Transfer of Ferrofluids Over A Horizontal Flat Plate with Leading Edge Accretion." *Journal of Advanced Research in Fluid Mechanics and Thermal Sciences* 59, no. 2 (2019): 163-181.
- [31] Aman, Sidra, Ilyas Khan, Zulkhibri Ismail, Mohd Zuki Salleh, and Qasem M. Al-Mdallal. "Heat transfer enhancement in free convection flow of CNTs Maxwell nanofluids with four different types of molecular liquids." *Scientific reports* 7, no. 1 (2017): 2445. <https://doi.org/10.1038/s41598-017-01358-3>
- [32] Ögüt, Elif Büyük, and Kamil Kahveci. "Mixed convection heat transfer of ethylene glycol and water mixture based Al₂O₃ nanofluids: effect of thermal conductivity models." *Journal of Molecular Liquids* 224 (2016): 338-345. <https://doi.org/10.1016/j.molliq.2016.09.075>